

# *Chandra* monitoring of UGC 4203: the structure of the X-ray absorber

G. Risaliti,<sup>1,2</sup> M. Elvis,<sup>2</sup> S. Bianchi<sup>3</sup>, G. Matt<sup>3</sup>

<sup>1</sup> *INAF - Osservatorio Astrofisico di Arcetri, L.go E. Fermi 5, Firenze, Italy*

<sup>2</sup> *Harvard-Smithsonian Center for Astrophysics, 60 Garden St. Cambridge, MA 02138 USA E-mail: grisaliti@cfa.harvard.edu*

<sup>3</sup> *Dipartimento di Fisica, Università degli Studi “Roma Tre”, Via della Vasca Navale 84, I-00146 Roma, Italy*

Released Xxxx Xxxxx XX

## ABSTRACT

We present a *Chandra* monitoring campaign of the highly variable Seyfert galaxy UGC 4203 (the “Phoenix Galaxy”) which revealed variations in the X-ray absorbing column density on time scales of two weeks. This is the third, clear case, after NGC 1365 and NGC 7582, of dramatic  $N_H$  variability on short time scales observed in a “changing look” source, i.e. an AGN observed in the past in both a reflection-dominated and a Compton-thin state. The inferred limits on the distance of the X-ray absorber from the center suggest that the X-ray “torus” could be one and the same with the broad emission line region. This scenario, first proposed for an “ad-hoc” picture for NGC 1365, may be the common structure of the circumnuclear medium in AGN.

**Key words:** Galaxies: AGN — Galaxies: individual (UGC 4203)

## 1 INTRODUCTION

The structure, size and composition of the circumnuclear medium of Active Galactic Nuclei (AGN) is the subject of several studies at different wavelengths. In particular, X-ray absorption variability has proven to be a powerful tool in order to establish the physical properties of the X-ray absorber/reflector: the almost ubiquitous absorption variability detected in bright absorbed AGN (Risaliti et al. 2002) is in itself an indication of a clumpy structure of the absorber. The time scale of such variations provide constraints on the dimensions and the distance from the central black hole of the obscuring clouds, under the assumption of Keplerian motion. The best characterization so far of the physical parameters of the X-ray absorber has been possible for the AGN in NGC 1365. This source has been monitored several times in the last few years with *Chandra*, *XMM-Newton*, *Suzaku*, and showed extreme variability in the X-rays: changes from Compton-thick to Compton-thin states on time scales from weeks (Risaliti et al. 2005) to days (Risaliti et al. 2007) to  $\sim 10$  hours (Risaliti et al. 2009A) and eclipses due to Compton-thin clouds ( $N_H \sim$  a few  $10^{23}$   $\text{cm}^{-2}$ ) on similar time scales (Risaliti et al. 2009B). These observations strongly support the view of an X-ray absorber made of clouds with  $N_H$  from  $10^{23}$  to  $>10^{24}$   $\text{cm}^{-2}$ , densities  $10^{10}$ - $10^{11}$   $\text{cm}^{-3}$  and distance from the center of hundreds of gravitational radii. These are all values typical of the broad emission line clouds (BELC). The global picture emerging for NGC 1365 is therefore quite different from the standard

view of the AGN unified models (Antonucci 1993): here, the X-ray absorber seems not to be associated to the parsec-scale dusty “torus” (Krolik & Begelman 1988) obscuring the BELC, but to the BELC themselves.

This scenario appears quite well justified for the single case of NGC 1365, whose extreme variability is so far unique among AGN. Two explanations of this uniqueness are possible: (1) NGC 1365 is intrinsically different from (most of) the other AGN; (2) NGC 1365 is an “average” AGN with favourable observational conditions (e.g. a particular line of sight through a torus made of clouds of different  $N_H$ , as in Risaliti et al. 2005).

In order to investigate this issue, the obvious strategy is to look for similar variations in other obscured AGN.

The most extreme known cases of spectral variations in AGN are those of the “changing look” AGN (Matt et al. 2003), i.e. sources with past X-ray observations in both a Compton-thin and a reflection-dominated state. Members of this class, besides NGC 1365, are NGC 6300 (Guainazzi. 2002), UGC 4203 (Guainazzi et al. 2002), NGC 2992 (Gilli et al. 2000), NGC 7674 (Bianchi et al. 2005), NGC 7582 (Piconcelli et al. 2007). In the latter case, a recent *Suzaku* campaign revealed  $N_H$  variations in time scales of a day (Bianchi et al. 2009), making NGC 7582 a second case of a “changing look” AGN with fast  $N_H$  variability.

The main open question about these sources is whether the observed dramatic spectral changes are due to variability

**Table 1.** Spectral parameters from past X-ray observations

Instr.	Date	Counts	$F_X^a$	$\Gamma^b$	$N_H^c$
ASCA	18/11/95	320	$0.2^e$	$2.0^d$	–
XMM	05/05/01	$>10^4$	2.6	$2.0^{+0.2}_{-0.2}$	$2.1^{+0.2}_{-0.2}$
Suzaku	27/05/07	$>10^4$	1.4	$1.9 \pm 0.2$	$3.3^{+0.2}_{-0.2}$
Swift 1	06/10/06	88	$1.6 \pm 0.4$	$1.9^d$	$1.7^{+0.5}_{-0.4}$
Swift 2	22/01/07	32	$1.2 \pm 0.5$	$1.9^d$	$2.5^{+1.5}_{-1.0}$
Swift 3	25/02/07	43	$0.9 \pm 0.5$	$1.9^d$	$1.9^{+1.0}_{-0.6}$
Swift 4	29/04/08	35	$2.3 \pm 0.8$	$1.9^d$	$3.4^{+1.2}_{-1.6}$

Results from past hard X-ray observations of UGC 4203. *a*: 2–10 keV unabsorbed flux, in units of  $10^{-11}$  erg s $^{-1}$  cm $^{-2}$ ; *b*: 2–10 keV photon index; *c*: absorbing column density, in units of  $10^{23}$  cm $^{-2}$ ; *d*: fixed. *e*: flux of the observed reflection-dominated spectrum. References: ASCA and XMM: Guainazzi et al. 2002; *Swift*: this work; *Suzaku*: Matt et al. 2009.

of the intrinsic emission or of the circumnuclear absorber. The case of NGC 2992 is clear: multiple observations on a  $\sim 20$  years period strongly suggest an intrinsic fading of the X-ray source (Gilli et al. 2000). We note that this is the only case among the “changing look” sources with a column density in the Compton-thin state of the order of  $10^{22}$  cm $^{-2}$ , while the other sources have  $N_H > 10^{23}$  cm $^{-2}$ .

Here we present the results of a *Chandra* monitoring campaign of one of the three remaining sources, UGC 4203 (other names: MKN 1210 and “Phoenix Galaxy”). Another *Chandra* campaign on one of the last two sources, NGC 6300, will be discussed in a future paper.

## 2 PAST OBSERVATIONS

UGC 4203 has been observed several times in the hard X-rays. The two observations which led to its classification as a “changing look” AGN, reported in Guainazzi et al. 2002, were performed with ASCA in 1998 and *XMM-Newton* in 2001. A further observation, has been performed simultaneously with *XMM-Newton* by *BeppoSAX*. More recently, the source has been observed with *Suzaku* in 2007, and with *Swift-XRT* for four times between 2006 and 2007. In order to obtain a complete view of the variability history of UGC 4203, we analyzed the *Swift-XRT* short observations (about two ks each) in order to estimate the flux and, if possible, the basic spectral parameters. We followed the standard procedure suggested by the *Swift* Data Center for the reduction and calibration. In all cases the net 2–10 keV spectral counts are below 100, allowing only a basic spectral analysis.

A summary of the spectral parameters obtained in these observations, assuming an absorbed power law model, is shown in Table 1.

## 3 CHANDRA OBSERVATIONS: REDUCTION AND ANALYSIS

The five 10 ks observations were performed with the ACIS-S instrument on-board *Chandra* between January 15 and February 06, 2008. The first three observations are almost consecutive, the fourth one is about two days after, and the fifth 17 days after the fourth.

We reduced and analyzed the data using the CIAO 4.2 package, and the most updated calibrations, following the standard procedure developed by the *Chandra* Data Center<sup>1</sup>. The background was extracted in an empty region in the ACIS-S field of view. The data were checked for possible alterations due to pile-up. Despite the high unabsorbed flux of the source (of the order of  $10^{-11}$  erg s $^{-1}$  cm $^{-2}$ ), no significant pile-up is expected, since the soft ( $< 3$  keV) photons from the AGN are absorbed by a column density of the order of  $2\text{--}3 \times 10^{23}$  cm $^{-2}$ . The spectral analysis has been performed with the Xspec 12 package (Arnaud et al. 1996).

A visual inspection of the five spectra (Fig. 1A, B) reveals a soft component at  $E < 2$  keV constant within a few per cent, and a second, hard component at  $E > 2$  keV with clear, strong variations between the fifth observation and the others.

We fitted the five spectra separately with a model consisting of the following components:

1. a soft spectrum produced by collisionally-ionized diffuse gas, with two different temperatures and densities (modeled through the APEC model<sup>2</sup> in XSPEC), and a power law, representing a possible scattering component from the central AGN. Our aim is to obtain a statistically acceptable representation of the soft emission, in order to fix it in the analysis of the variability of the hard component. An alternative, simpler approach would be an analysis of the spectrum at energies  $E > 3$  keV, neglecting the soft part of the spectrum. This would however prevent us from rejecting models reproducing the hard spectrum, but whose extrapolation at low energies over-predicts the observed counts. The fitting analysis shows that all the three components are needed to obtain a good representation of the observed data. The thermal component has a temperature  $kT = 0.7 \pm 0.2$  keV and the power law slope and normalizations are  $\Gamma_S = 2.05 \pm 0.15$  and  $N_S = 2.0^{+0.4}_{-0.3} \times 10^{-5}$  keV s $^{-1}$  cm $^{-2}$  keV $^{-1}$  (corresponding to a flux of a few per cent of that of the intrinsic AGN continuum, see below). These are all typical parameters for the soft emission of local AGN. The metallicities of the photoionized component span a large range (from 0.5 to 20 solar) and are poorly constrained. This is analogous to what is obtained in global fits of the soft diffuse emission of other AGN. A spatially resolved analysis of these cases, when possible (i.e. in lower-redshift sources) show that the total soft emission is the result of the contributions of different zones in the galactic bulge with a large range of metallicities and densities (e.g. Baldi et al. 2006, Wang et al. 2009). Since we were interested in the hard component, we froze the soft components to their best fit parameters in the subsequent analysis.
2. An intrinsic AGN emission consisting of an absorbed power law. The absorption is modeled with a single photoelectric component, and then with a double component, one of which partially covering the source (see below for details).
3. A cold reflection component, consisting of a continuum estimated with the XSPEC PEXRAV model (Magdziar &

<sup>1</sup> <http://cxc.harvard.edu/ciao/index.html>

<sup>2</sup> <http://cxc.harvard.edu/atomdb/>

**Table 2.** Results from the spectra analysis of *Chandra* data

Group	$\Gamma$	$N_H^a$	R <sup>b</sup>	F <sup>c</sup>	$\chi^2/\text{d.o.f.}$
Independent fits					
OBS 1-3	$1.83^{+0.47}_{-0.47}$	$32^{+7}_{-7}$	$1.7^{+1.7}_{-0.8}$	2.2	176/215
OBS 4	$0.64^{+0.78}_{-0.53}$	$14.7^{+2.3}_{-3.1}$	<7	1.1	62/64
OBS 5	$0.77^{+0.66}_{-0.68}$	$21^{+12}_{-6}$	<8	1.1	51/49
Constant reflection, $1.7 < \Gamma < 2.2$					
OBS 1-3	1.7-2.2	$29.6^{+1.8}_{-1.7}$	$1.5^{+1.0}_{-1.0}$	1.8	306/326
OBS 4	1.7-2.2	$25.5^{+3.3}_{-2.9}$	$2.0^{+1.1}_{-1.0}$	1.4	306/326
OBS 5	1.7-2.2	$37.6^{+4.4}_{-4.6}$	$1.9^{+2.0}_{-1.5}$	1.4	306/326

<sup>a</sup> Column density in units of  $10^{23} \text{ cm}^{-2}$ . <sup>b</sup>: Ratio between the intrinsic continuum assumed in the reflection component and the observed continuum. <sup>c</sup>: unabsorbed 2-10 keV flux, in units of  $10^{-11} \text{ erg cm}^{-2} \text{ s}^{-1}$ .

Zdziarski 1995) and an iron emission line.

Since the spectral fits confirmed that no significant variation is present among the first three almost consecutive observations, we repeated the analysis linking the parameters in these intervals. Hereinafter, we use the names OBS 1-3, OBS 4, and OBS 5 to refer to the three groups considered in the analysis.

The results from the spectral fitting are reported in Table 2 (top). Even if the models are acceptable from a statistical point of view ( $\chi^2_\nu \sim 1$  for all the spectra), the present analysis is not satisfactory for two reasons:

1) the best fit continuum in the fourth and fifth interval is extremely flat ( $\Gamma \sim 0.7$ ). Such a flat photon index has not been observed thus far in any non-reflection dominated AGN (see, e.g. the distribution of  $\Gamma$  in nearby AGN in Bianchi et al. 2009A, or Dadina et al. 2008), and is therefore unlikely to be real. Moreover, all the previous spectra of UGC 4203 with high statistics (Table 1), and the combined *Chandra* spectra of the first three interval, also having a much higher signal-to-noise, are well fitted with a fairly “normal” photon index, in the range 1.7-2.2.

2) The spectral parameters in OBS 4 and OBS 5 are poorly constrained, due to the high degeneracy between photon index, column density and reflection component. This is evident from the large errors reported in Table 2. However, the  $\Gamma$ - $N_H$  contour plots (Fig. 2), show that a constant solution for all the intervals is ruled out at high statistical significance.

In order to overcome these limitations and better constrain the spectral parameters, we repeated the spectral analysis fitting all the interval simultaneously, and requiring a) a constant reflection component, and b) a continuum photon index in the range 1.7-2.2. Not surprisingly (given the large contours in Fig. 2) the overall fit is completely satisfactory ( $\chi^2=306/324$  d.o.f.). The results are listed in Table 2 (bottom) and shown in Fig. 3. Both variations in intrinsic flux and in absorbing column density are necessary to explain the observed spectral variations. With these prescriptions, treating the three column densities as independent, the probability of having no column density variation is  $P(\Delta N_H=0) < 10^{-3}$ . Specifically, the measured column densities in OBS 1-3 and OBS 4 are consistent, while the column density from the fifth observation,  $N_H(\text{OBS 5})$ , is different from  $N_H(\text{OBS 1-3})$  at a 99.5% confidence level, and from

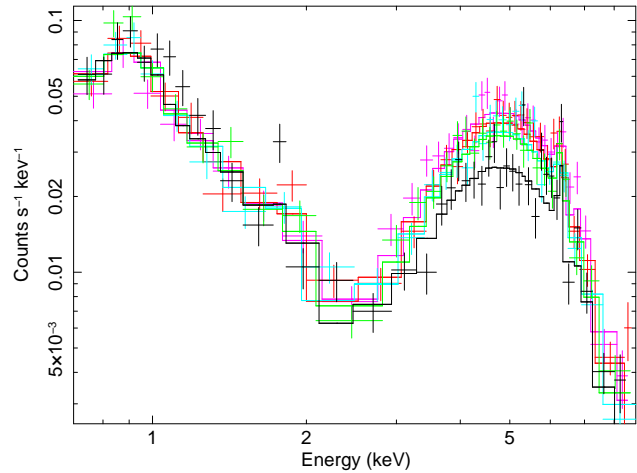


**Figure 1.** *Chandra* 0.5-10 keV spectra of UGC 4203. Note that the soft ( $E < 2$  keV) and hard ( $E > 7$  keV) emission is constant within a few percent in all the five observations, while significant variations occurred in the 2-6 keV range between the first four observations and the fifth one (in black).

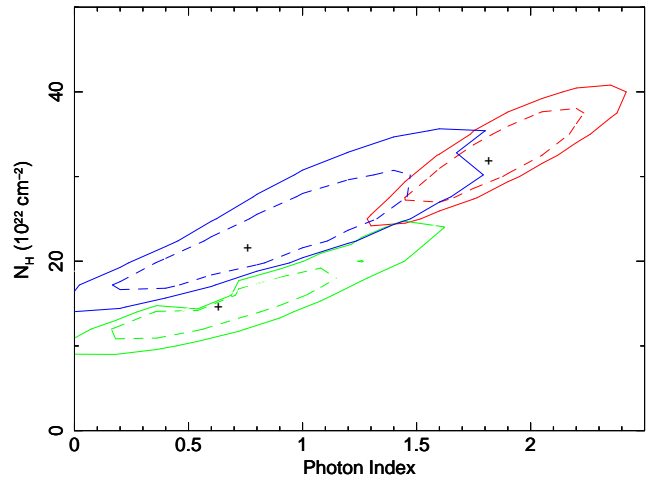


**Figure 2.** Photon index- $N_H$  1- and 2- $\sigma$  contours for OBS 1-3 (red), OBS 4 (green) and OBS 5 (blue).

$N_H(\text{OBS 4})$  at a 99.98% confidence level. The latter is the statistically most significant difference. The contour plot for  $N_H(\text{OBS 4})$  and  $N_H(\text{OBS 5})$  are shown in Fig. 4.

Finally, repeating the fit assuming constant column density between OBS 1-3 and OBS 4, we obtain  $N_H(\text{OBS 1-4}) = 29.2^{+1.5}_{-1.7} \times 10^{23} \text{ cm}^{-2}$ , and  $N_H(\text{OBS 5}) = 37.7^{+5.2}_{-4.6} \times 10^{23} \text{ cm}^{-2}$ . The probability of no column density variation is obtained imposing  $N_H(\text{OBS 5}) = N_H(\text{OBS 1-4})$ .  $P(\Delta N_H=0) = 3 \times 10^{-3}$ .

We conclude that the column density variability between OBS 5 and the previous intervals is highly significant. Changes in intrinsic flux are also present, and the continuum spectral slope may be also variable (within a physically acceptable range), but these components alone cannot reproduce the observations without a variable absorber.

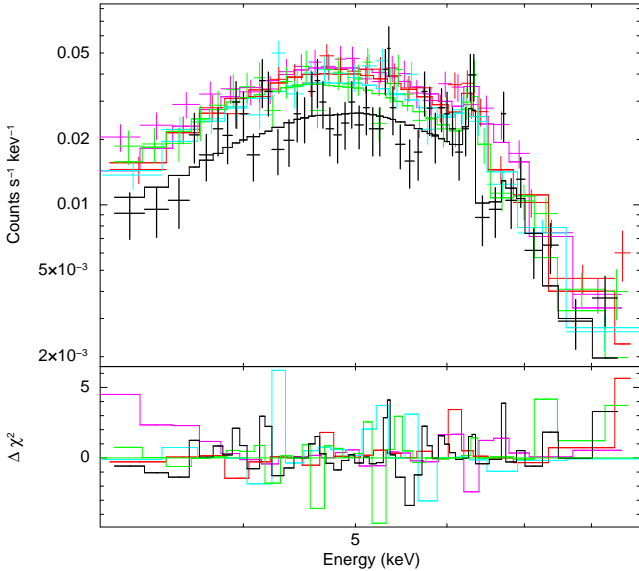


**Figure 3.** 3-10 keV spectrum, best fit model and  $\chi^2$  residuals for the five *Chandra* observations.

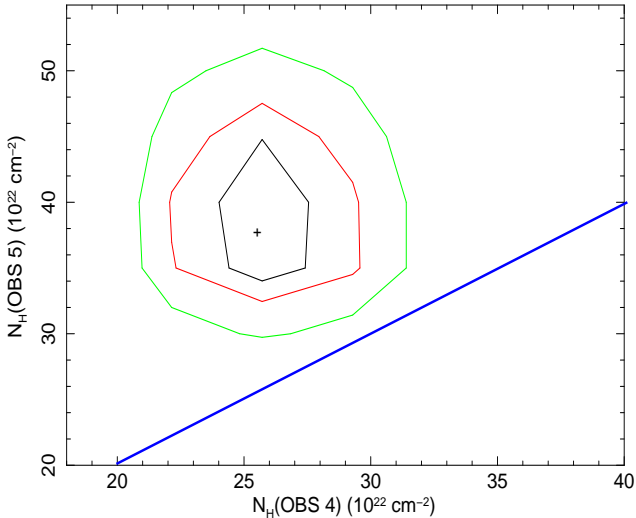


**Figure 4.** Column density contours (1, 2 and 3  $\sigma$ ) from the best fit models to OBS 4 and OBS 5. The equal column density line is also plotted, for ease of comparison.

#### 4 THE STRUCTURE OF THE X-RAY ABSORBER

The results of our analysis show a column density variation in a time scale  $\Delta T$  between 3 days (the time between the first and the fourth observation, during which no variation has been found) and 17 days. This result presents a strong resemblance to the column density variations found in the analogous *Chandra* campaign on NGC 1365 (Risaliti et al. 2007). Therefore, in the following we apply the same analysis as for NGC 1365.

The variability time scale can be easily translated into an estimate of the distance of the absorbing cloud, assuming a rotation around the central black hole (BH) with Keplerian velocity  $V_K$ . This estimate is subject to large uncertainties, connected to the values of the BH mass,

and of the cloud velocity, which are discussed below.

**Black hole mass.** An estimate of the BH mass  $M_{BH}$  can be obtained from the known relations between  $M_{BH}$  and spectral lines, bulge luminosity, and bulge velocity dispersion. In the case of UGC 4203, discrepant estimates are found in the literature:

1)  $M_{BH}$ - $\sigma$  relation. The relatively low bulge velocity dispersion ( $\sigma=77$  km s $^{-1}$ , Garcia-Rissmann et al. 2005) suggests  $\log(M_{BH}/M_{\odot})\sim 6.5$  (Bian & Gu 2007). The value obtained from the velocity dispersion imply a super-Eddington luminosity, if a standard X-ray to bolometric correction is adopted, based on known Quasar Spectral Energy Distributions (e.g. Risaliti & Elvis 2004), and the relation between optical to X-ray ratio and UV luminosity (Young et al. 2009). We consider this scenario highly unlikely, mainly because of the rather constant intrinsic X-ray flux (within a factor  $\sim 2$  of the one measured with *Chandra*, Table 1 and 2) over several years, which would imply a persistent super- or near-Eddington luminosity for this long period. On the other hand, the estimate of  $M_{BH}$  based on velocity dispersions may be strongly biased in this case by the presence of an unusually strong starburst in the bulge of UGC 4203 (Mazzalay & Rodríguez-Ardila 2007).

2)  $M_{BH}$ -bulge luminosity relation. We estimated  $M_{BH}$  using the Marconi & Hunt (2003) relation between H-band bulge magnitudes and BH masses, using the 2MASS H magnitude in the inner 4 kpc of the galaxy, and the ratio between AGN and stellar contribution in H-band estimated by Mazzalay & Rodríguez-Ardila (2007). We obtain  $\log(M_{BH}/M_{\odot})\sim 7.7$ .

3) Virial mass estimates. The reverberation mapping-calibrated relation of Vestergaard et al. (2006) suggests  $\log(M_{BH}/M_{\odot})\sim 7.9$  (Zhang et al. 2008). In this estimate the width of the broad H $\beta$  line is measured in the polarized spectrum, while the intrinsic luminosity at 5100 Å is estimated from the [O III]  $\lambda 5007$  Å line. - The [O III]-based luminosity is confirmed by an analogous estimate based on the intrinsic X-ray luminosity, following the same prescriptions as mentioned above. The measurement of FWHM(H $\beta$ ) is also quite solid, being based on a rather high quality spectrum (Tran 1995).

Concluding, despite the large uncertainties in each of the methods summarized above, we assume  $M_{BH}\sim 5\text{--}7\times 10^7 m_{\odot}$  as the most likely mass estimate.

**Cloud velocity.** the linear dimension of the X-ray source cannot be lower than a few gravitational radii,  $R_G=GM_{BH}/c^2$ . Adopting  $D_S\sim 5 R_G$  as a lower limit, the velocity of the eclipsing cloud must therefore satisfy the condition:  $V_K\times\Delta T>5 R_G$ . Adopting the mass estimate discussed above, this translates into  $V_K>10^3$  km s $^{-1}$   $\Delta T_{10}$ , where  $\Delta T_{10}$  is the time interval in units of 10 days. This value is clearly in the range of the Broad Emission Line Clouds (BELCs) and well above that typical of the standard, parsec-scale obscuring torus.

#### 4.1 Physical properties

Based on the above estimates, and assuming Keplerian motion of the obscuring cloud, we obtain a distance from the

central black hole  $R \sim 1-2 \times 10^{17}$  cm. The cloud linear size  $D_C$  must be of the order of, or a few times larger, than that of the X-ray source, i.e.  $D_C \sim 1-5 \times 10^{14}$  cm. The measured column density  $N_H \sim 10^{23}$   $\text{cm}^{-2}$  imply a density of the order of  $10^9$   $\text{cm}^{-3}$ .

We conclude that the X-ray absorber has all the typical physical parameters of a Broad Line Region cloud. Therefore, absorption in X-rays and the broad optical/UV emission lines are most likely due to the same physical component. We also note that UGC 4203 is optically classified as a type 2 source, implying the presence of dust along the line of sight. This dust cannot be associated to the Broad Line Region, which is well inside the dust sublimation radius, and must therefore be located in a farther absorber. The nature of this second absorber may be a galactic dust lane, and/or a "classical" parsec-scale torus. In either case, a contribution to the observed X-ray absorption by this second component is expected. Within the limited statistics of our *Chandra* observations it is not possible to disentangle these two components in the spectral fits. The contribution to the observed column density may be as low as a few  $10^{22}$   $\text{cm}^{-2}$ , or as high as the lowest  $N_H$  measured in past observations, i.e.  $\sim 2 \times 10^{23}$   $\text{cm}^{-2}$  (Table 1).

UGC 4203 is one more "Changing look" AGN where the extreme X-ray variability is proven to be due to absorption by BLR clouds. The same conclusion can be reached for a few more sources where a similar variability has been found (NGC 4151, Puccetti et al. 2007, NGC 4388, Elvis et al. 2004, NGC 7582, Bianchi et al. 2009B, Mrk 766, Risaliti et al. 2009). On the other hand, it is likely that other bright sources with multiple X-ray observations do not show short-term absorption variability (even if no quantitative analysis has been done so far), and that other sources of X-ray absorption, quite far from the central source, may be present (e.g., as discussed above, galactic dust lanes and/or parsec-scale tori). Therefore, since the physical link between BLR clouds and X-ray absorber has been now established for a good number of sources, our next step will be the complete analysis of a representative sample, in order to quantitatively estimate the relevance of short term variable X-ray absorption in local AGN.

**ACKNOWLEDGEMENTS**

This research has made use of data obtained from the Chandra Data Archive and the Chandra Source Catalog, and software provided by the Chandra X-ray Center (CXC). This work has been partially funded by NASA grants G08-9107X and G09-0105X.

**REFERENCES**

Arnaud, K. A. 1996, *Astronomical Data Analysis Software and Systems V*, 101, 17

Baldi A., Raymond J. C., Fabbiano G., Zezas A., Rots A. H., Schweizer F., King A. R., Ponman T. J., 2006, *ApJS*, 162, 113

Bian W., Gu Q., 2007, *ApJ*, 657, 159

Bianchi S., Guainazzi M., Matt G., Fonseca Bonilla N., Ponti G., 2009A, *A&A*, 495, 421

Bianchi S., Piconcelli E., Chiaberge M., Bailón E. J., Matt G., Fiore F., 2009B, *ApJ*, 695, 781

Gilli, R., Maiolino, R., Marconi, A., Risaliti, G., Dadina, M., Weaver, K. A., & Colbert, E. J. M. 2000, *A&A*, 355, 485

Krolik, J. H. & Begelman, M. C. 1988, *ApJ*, 329, 702

Dadina M., 2008, *A&A*, 485, 417

Elvis M., Risaliti G., Nicastro F., Miller J. M., Fiore F., Puccetti S., 2004, *ApJ*, 615, L25

Garcia-Rissmann A., Vega L. R., Asari N. V., Cid Fernandes R., Schmitt H., González Delgado R. M., Storchi-Bergmann T., 2005, *MNRAS*, 359, 765

Guainazzi M., Matt G., Fiore F., Perola G. C., 2002, *A&A*, 388, 787

Guainazzi M., 2002, *MNRAS*, 329, L13

Magdziarz, P. & Zdziarski, A. A. 1995, *MNRAS*, 273, 837

Marconi A., Hunt L. K., 2003, *ApJ*, 589, L21

Matt, G., Guainazzi, M., & Maiolino, R. 2003, *MNRAS*, 342, 422

Matt G., Bianchi S., Awaki H., Comastri A., Guainazzi M., Iwasawa K., Jimenez-Bailon E., Nicastro F., 2009, *A&A*, 496, 653

Mazzalay X., Rodríguez-Ardila A., 2007, *A&A*, 463, 445

Piconcelli E., Bianchi S., Guainazzi M., Fiore F., Chiaberge M., 2007, *A&A*, 466, 855

Puccetti, S., Fiore, F., Risaliti, G., Capalbi, M., Elvis, M., & Nicastro, F. 2007, *MNRAS*, 377, 607

Risaliti, G., Elvis, M., & Nicastro, F. 2002, *ApJ*, 571, 234

Risaliti G., Elvis M., 2004, *ASSL*, 308, 187

Risaliti, G., Elvis, M., Fabbiano, G., Baldi, A., & Zezas, A. 2005a, *ApJ*, 623, L93 (R05A)

Risaliti, G., Elvis, M., Fabbiano, G., Baldi, A., Zezas, A., & Salvati, M. 2007, *ApJ*, 659, L111

Risaliti G., et al., 2009A, *MNRAS*, 393, L1

Risaliti G., et al., 2009B, *ApJ*, 696, 160

Young M., Elvis M., Risaliti G., 2009, arXiv, arXiv:0911.0474

Zhang S.-Y., Bian W.-H., Huang K.-L., 2008, *A&A*, 488, 113

Wang J., Fabbiano G., Elvis M., Risaliti G., Mazzarella J. M., Howell J. H., Lord S., 2009, *ApJ*, 694, 718